

Computer simulations of polydisperse ER fluids in DID model

Andrew C. T. Wong¹, Hua Sun^{1,2} and K. W. Yu¹

¹*Department of Physics, The Chinese University of Hong Kong, Shatin, NT, Hong Kong*

²*Department of Physics, Suzhou University, Suzhou 215006, China*

Abstract

The theoretical investigations on electrorheological (ER) fluids are usually concentrated on monodisperse systems. Real ER fluids must be polydisperse in nature, i.e., the suspended particles can have various sizes and/or different dielectric constants. An initial approach for these studies would be the point-dipole (PD) approximation, which is known to err considerably when the particles approach and finally touch due to multipolar interactions. In a recent work, we proposed a dipole-induced-dipole (DID) model for computer simulation of ER fluids, which was shown to be both more accurate than the PD model and easy to use. The DID model was applied to simulate the athermal aggregation of particles in ER fluids and the aggregation time was found to be significantly reduced as compared to the PD model. In this work, we will report results for the case when the dielectric contrasts of some particles can be negative. In which case, the direction of the force is reversed. Moreover, the inclusion of DID force further complicates the results because the symmetry between positive and negative contrasts will be broken by the presence of dipole-induced interactions.

PACS Number(s): 83.80.Gv, 82.70.-y, 42.20.-q

Typeset using REVTeX

I. INTRODUCTION

Many theoretical investigations on electrorheological (ER) fluids are usually concentrated on monodisperse systems in which all the suspended particles are of the same size and dielectric constant. In reality ER fluids must be polydisperse in nature, i.e., the particles can have various sizes and/or different dielectric permittivities [1]. For instance, the particle size has a significant impact on the yield stress [2], as well on the rheology [3]. An initial approach for these studies would be the point-dipole (PD) approximation [4]. As many-body and multipolar interactions between the particles have been neglected, the PD approximation is known to err considerably when the particles approach and finally touch. The PD approximation becomes even worse when the dielectric contrasts between the suspended particles and the host medium become large. To circumvent the problem, we recently employed the multiple image method to compute the interparticle force for a polydisperse ER fluid [5]. From the results, we proposed a dipole-induced-dipole (DID) model for computer simulations of ER fluids; the DID model yields very good agreements with the multiple image results for a wide range of dielectric contrasts and polydispersity [5]. The DID model has recently been employed to simulate the athermal aggregation of particles in ER fluids in which the particles are of different permittivities [6]. Moreover, the dielectric contrasts between the particles and the host fluids were all positive. The aggregation time was found to be significantly reduced, both in uniaxial and rotating electric fields [6]. In this work, we will report results for the case when the dielectric contrasts of some particles can be negative. In which case, the direction of the force should be reversed [7]. The inclusion of the DID force further complicates the results because the symmetry between positive and negative contrasts will be broken by the presence of dipole-induced interactions. We found that the aggregation time can be much increased as compared to the PD model.

In the next section, we review the multiple image method and establish the DID model. In section III, we apply the DID model to the computer simulation of ER fluids in a uniaxial field. In section IV, we extend the simulation to athermal aggregation in rotating fields.

Discussion on our results will be given.

II. MULTIPLE IMAGE METHOD

In this section, we generalize the multiple image method [5] to handle both positive and negative dielectric contrasts. Consider a pair of dielectric spheres, of radii a and b , dielectric constants ϵ_1 and ϵ'_1 respectively, separated by a distance r . The spheres are embedded in a host medium of a dielectric constant ϵ_2 . Upon the application of an electric field \mathbf{E}_0 , the induced-dipole moment inside the spheres are, respectively, given by (SI units)

$$p_{a0} = 4\pi\epsilon_0\epsilon_2\beta E_0 a^3, \quad p_{b0} = 4\pi\epsilon_0\epsilon_2\beta' E_0 b^3, \quad (1)$$

where the dipole factors β, β' are defined as

$$\beta = \frac{\epsilon_1 - \epsilon_2}{\epsilon_1 + 2\epsilon_2}, \quad \beta' = \frac{\epsilon'_1 - \epsilon_2}{\epsilon'_1 + 2\epsilon_2}. \quad (2)$$

In the point-dipole (PD) model, the force between two particles is given by

$$\mathbf{F}_{PD} = \frac{F}{r^4} \left[(2 \cos^2 \theta - \sin^2 \theta) \hat{\mathbf{r}} + \sin 2\theta \hat{\boldsymbol{\theta}} \right], \quad (3)$$

where $F = 12\pi\epsilon_0\epsilon_2\beta\beta'a^3b^3E_0^2$, $\hat{\mathbf{r}}$ and $\hat{\boldsymbol{\theta}}$ are unit vectors. Many previous studies were concentrated on the case in which both $\beta, \beta' > 0$. When the β s adopt opposite signs, the direction of the PD force will be reversed. In a recent paper, we derived a correction to the PD force from the multiple image method [6]. The total dipole moment inside sphere a is

$$p_{aT} = (\sinh \alpha)^3 \sum_{n=1}^{\infty} \left[\frac{p_{a0}b^3(-\beta)^{n-1}(-\beta')^{n-1}}{(b \sinh n\alpha + a \sinh(n-1)\alpha)^3} + \frac{p_{b0}a^3(-\beta)^n(-\beta')^{n-1}}{(r \sinh n\alpha)^3} \right], \quad (4)$$

$$p_{aL} = (\sinh \alpha)^3 \sum_{n=1}^{\infty} \left[\frac{p_{a0}b^3(2\beta)^{n-1}(2\beta')^{n-1}}{(b \sinh n\alpha + a \sinh(n-1)\alpha)^3} + \frac{p_{b0}a^3(2\beta)^n(2\beta')^{n-1}}{(r \sinh n\alpha)^3} \right], \quad (5)$$

where the subscripts $T(L)$ denote a transverse (longitudinal) field, i.e., the applied field is perpendicular (parallel) to the line joining the centers of the spheres. Similar expressions for the total dipole moment inside sphere b can be obtained by interchanging a and b , as well as β and β' . The parameter α satisfies

$$\cosh \alpha = \frac{r^2 - a^2 - b^2}{2ab}. \quad (6)$$

The forces between the spheres is given by [8]

$$F_T = \frac{E_0}{2} \frac{\partial}{\partial r} (p_{aT} + p_{bT}), \quad F_L = \frac{E_0}{2} \frac{\partial}{\partial r} (p_{aL} + p_{bL}). \quad (7)$$

It should be noted that the multiple image results can be used to compare among the various models according to how many terms are retained in the multiple image expressions:

(a) PD model: $n = 1$ term only, (b) DID model: $n = 1$ to $n = 2$ terms only, and (c) multiple-induced-dipole (MID) model: $n = 1$ to $n = \infty$ terms.

For convenience, we define the reduced separation $\sigma = r/(a + b)$. Here we set $a = b$. We consider two cases: (a) $\beta > 0, \beta' < 0$ or $\epsilon_1 > \epsilon_2 > \epsilon'_1$ and (b) $\beta = \beta' < 0$ or $\epsilon_2 > \epsilon_1 = \epsilon'_1$. The interparticle forces in the longitudinal and transverse cases are plotted in Fig.1 with different values of the dielectric contrasts. For the case (a) depicted in Fig.1(a), the magnitude of MID force falls between that of the PD and DID in both the longitudinal and transverse cases. At low contrasts, the DID results almost coincide with the MID results. While at high contrast, the DID model exhibits significant deviation from MID when $\sigma < 1.1$. For the case (b) as depicted in Fig.1(b), the DID results almost coincide with the MID results at low contrast, while deviate significantly at high contrast. The forces are found to be qualitatively different from the case of $\beta, \beta' > 0$. Thus, by including the multiple image contributions, it is observed that the case of $\beta, \beta' < 0$ significantly different from the presumably symmetric case of $\beta, \beta' > 0$. The symmetry has been broken due to the presence of DID forces.

III. ATHERMAL AGGREGATION IN THE UNIAXIAL FIELD

The multiple image expressions [Eqs.(4) and (5)] allow us to calculate the correction factor defined as the ratio between the DID and the PD forces [6]:

$$\frac{F_{DID}^{(\parallel)}}{F_{PD}^{(\parallel)}} = 1 + \frac{2\beta a^3 r^5}{(r^2 - b^2)^4} + \frac{2\beta' b^3 r^5}{(r^2 - a^2)^4} + \frac{4\beta\beta' a^3 b^3 (3r^2 - a^2 - b^2)}{(r^2 - a^2 - b^2)^4}, \quad (8)$$

$$\frac{F_{DID}^{(\perp)}}{F_{PD}^{(\perp)}} = 1 - \frac{\beta a^3 r^5}{(r^2 - b^2)^4} - \frac{\beta' b^3 r^5}{(r^2 - a^2)^4} + \frac{\beta\beta' a^3 b^3 (3r^2 - a^2 - b^2)}{(r^2 - a^2 - b^2)^4}, \quad (9)$$

$$\frac{F_{DID}^{(\Gamma)}}{F_{PD}^{(\Gamma)}} = 1 + \frac{\beta a^3 r^3}{2(r^2 - b^2)^3} + \frac{\beta' b^3 r^3}{2(r^2 - a^2)^3} + \frac{3\beta\beta' a^3 b^3}{(r^2 - a^2 - b^2)^3}, \quad (10)$$

where $F_{PD}^{(\perp)} = 3p_{a0}p_{b0}/4\pi\epsilon_0\epsilon_2r^4$, $F_{PD}^{(\parallel)} = -6p_{a0}p_{b0}/4\pi\epsilon_0\epsilon_2r^4$, and $F_{PD}^{(\perp)} = -3p_{a0}p_{b0}/4\pi\epsilon_0\epsilon_2r^4$ are the point-dipole forces for the transverse, longitudinal, and Γ cases, respectively. If we denote the ratios in Eqs.(8)–(10) by K_{\parallel} , K_{\perp} and K_{Γ} respectively, the force between two particles is modified to

$$\mathbf{F}_{DID} = \frac{F}{r^4} \left[(2K_{\parallel} \cos^2 \theta - K_{\perp} \sin^2 \theta) \hat{\mathbf{r}} + K_{\Gamma} \sin 2\theta \hat{\boldsymbol{\theta}} \right].$$

In what follows, we consider two spheres of equal radius a and various dipole factors β and β' respectively. These spheres are initially at rest and at a separation d_0 . For aggregation induced by a uniaxial field, we consider two cases. For case (a) $\beta > 0, \beta' < 0$ or $\epsilon_1 > \epsilon_2 > \epsilon'_1$, the electric field is perpendicular to the line joining the centers of the spheres. The equation of motion is given by

$$\frac{dz}{dt} = F_{\perp}(2z), \quad (11)$$

while for case (b) $\beta = \beta' < 0$ or $\epsilon_1 = \epsilon'_1 < \epsilon_2$, the electric field is parallel to the line joining the centers of the spheres. The equation of motion becomes

$$\frac{dz}{dt} = F_{\parallel}(2z), \quad (12)$$

where z is the displacement of one sphere from the center of mass. The separation between the two spheres is therefore $d = 2z$ and the initial condition is $d = d_0$ at $t = 0$. Eqs.(11) and (12) are dimensionless equation. Following Klingenberg and with slight modification, we choose the following natural scaling units to define the dimensionless variables [4]:

$$z_0 = 2a, \quad t_0 = 12\pi\eta_c a^2 / F_0, \quad F_0 = \frac{3}{4}\pi\epsilon_0\epsilon_2 E_0^2 a^2, \quad (13)$$

where E_0 is the field strength, m the mass, and η_c the coefficient of viscosity. We have followed Klingenberg to ignore the inertial effect and thermal motion of the particles [4]. The initial separation d_0 is related to the volume fraction ϕ by

$$\frac{d_0}{2a} = \left(\frac{\pi}{6\phi} \right)^{1/3}. \quad (14)$$

In the PD approximation, Eq.(11) admits an analytic solution

$$z = \left[\left(\frac{d_0}{4a} \right)^5 + \frac{5\beta\beta't}{16} \right]^{1/5}, \quad (15)$$

while Eq.(12) gives

$$z = \left[\left(\frac{d_0}{4a} \right)^5 - \frac{5\beta\beta't}{8} \right]^{1/5}. \quad (16)$$

It is obvious the above equations impose a condition for aggregation in uniaxial field, namely, the transverse case requires that β and β' are of different signs while the longitudinal case requires that they are of the same sign.

For the DID model, we integrate the equations of motion by the fourth-order Runge-Kutta algorithm, with the time step $\delta t = 0.0001$ for both small and large volume fractions. In Fig.2, we plot the reduced separation σ against dimensionless time t/t_0 . The results reveal that in general the DID results deviate slightly from the PD results at low volume fractions, i.e. at a large initial separation, while the deviation becomes large at high volume fractions. The deviations are more pronounced at high contrasts, attributed to a large attractive force, resulting in a smaller aggregation time. In both cases (a) and (b), the DID aggregation time is generally larger than that of PD. While in the case $\beta, \beta' > 0$, the situation is reversed. This feature can be understood from the force magnitudes of the two models (see Fig.1).

Fig.3 shows the ratio of the aggregation time for the PD model to the DID model against reduced initial separation $d_0/2a$. The aggregation time of the DID model is generally larger than that of the PD model especially when the initial separation is small. The correction factor is more pronounced at high contrast. In the case $\beta = \beta' < 0$ or $\epsilon_2 > \epsilon_1 = \epsilon'_1$, we observe a non-monotonic dependence, the correction factor increases significantly when the spheres are close and decrease again when $d/2a = 1.13$ or less at high contrast. This behavior can be understood from the interparticle force (Fig.1(b), the three panels on the right). At low contrast, the difference in magnitude between the PD and DID force increases

monotonically as the separation decreases. However at high contrast the difference increases first then decreases again as the separation decreases.

IV. ATHERMAL AGGREGATION IN THE ROTATING FIELD

Perhaps it is more interesting to consider aggregation in a rotating electric field [6]. Consider a rotating field applied in the x - y plane, $E_x = E_0 \cos \omega t$, $E_y = E_0 \sin \omega t$. The dimensionless equation of motion for the two spheres becomes

$$\frac{dx}{dt} = F_{\parallel}(r) \cos^2 \omega t + F_{\perp}(r) \sin^2 \omega t, \quad \frac{dy}{dt} = -F_{\Gamma}(r) \sin 2\omega t \quad (17)$$

where (x, y) are the displacement of one sphere from their center of mass and $r = 2\sqrt{x^2 + y^2}$ is the separation between two particles. In case of a large ω , we may safely neglect the y direction of the motion. For the PD approximation, the dimensionless forces are $F_{\parallel} = -2\beta\beta'/r^4$ and $F_{\perp} = \beta\beta'/r^4$, respectively, which yields the analytic solution

$$x = \left[\left(\frac{d_0}{4a} \right)^5 - \frac{5\beta\beta'}{64\omega} (\omega t + 3 \sin 2\omega t) \right]^{1/5} \quad (18)$$

The separation between two spheres is $d = 2x$. For the DID model, we integrate the equation of motion by the fourth-order Runge-Kutta algorithm, with a time step $\delta t = 1/400\omega$.

Note that the two particles cannot aggregate if $\beta > 0, \beta' < 0$ or $\epsilon_1 > \epsilon_2 > \epsilon'_1$ in the rotating field because the repulsive force induced by longitudinal field F_L is always larger than the attractive force induced by transverse field F_T , while the particles spend equal times in both fields on the average. The displacement-time graph of the aggregations with $\epsilon_2 > \epsilon_1 = \epsilon'_1$ in the two models are plotted in Fig.4. The shape of the displacement-time graph of DID model is different from that of the PD model, especially when the two spheres are close, resulting in a large deviation between the DID and PD models in the aggregation time. This behavior can again be understood by the interparticle force between the two spheres. We can see from Fig.1(b) that the DID longitudinal attractive force and its transverse repulsive force is about the same when the separation is small. Since the spheres

spend equal times in the longitudinal and transverse field and they change the direction of motion according to the rotating field, the displacement of the spheres can be estimated by the difference between the magnitude of the longitudinal attractive force and the transverse repulsive force, as there would be no displacement if the magnitude of the two forces are the same. Thus when the two spheres are near, their velocity become smaller and have different shape in the displacement-time graph. On the other hand, the PD attractive force is sufficiently larger than its repulsive force at any separation.

We further calculated the correction factor of the aggregation time for the PD model with respect to the DID model in the same way as in the uniaxial field case. We plot the correction factor against the reduced initial separation $d_0/2a$ with different parameters in Fig.5. The aggregation time is significantly increased when the mutual polarization of the two spheres is taken into account. The increase becomes even more pronounced and oscillating when the initial separation is small. The oscillation is due to the sensitive dependence on the initial polarization of dipoles when the spheres are close.

DISCUSSION AND CONCLUSION

Here a few comments on our results are in order. In this work, we have concentrated on the multipolar interactions between touching particles, which we believe are more important than the many-body or local-field effects [9,10]. In the latter approaches, the particles in ER fluids are still treated as point dipoles, while their dipole moments are determined by adding the local-field corrections. In the DID model, the additional terms arise from multipole interactions, rather than from local-field corrections.

We have studied the aggregation time for two spherical particles. We should also examine the morphology of aggregation in polydisperse ER fluids, due to the dipole-induced forces. To this end, it may be difficult to obtain the ground state lattice in polydisperse ER fluids by using dynamic simulations alone, since both body-centred tetragonal and simple cubic or even honeycomb stacking lattices coexist in such systems according to Kaski and coworkers

[11]. Moreover, many external factors such as the numbers of particles, the size of the cell, etc. will affect the final results. We are currently trying to incorporate the DID terms in the interaction energy. In this connection, we can also examine the recently proposed structural transformation by applying the uniaxial and rotating fields simultaneously to an ER fluid [12].

In summary, we have used the DID model to deal with computer simulations of polydisperse ER fluids for the case when the dielectric contrasts of some particles can be negative. We studied athermal aggregation of two spherical particles both in uniaxial and rotating electric fields. We showed that an inclusion of the DID force breaks the symmetry between positive and negative contrasts. As a result, the aggregation time can be much increased as compared to the PD model.

ACKNOWLEDGMENTS

This work was supported in part by the Direct Grant for Research, and in part by the RGC Earmarked Grant. K. W. Y. acknowledges useful discussion with Dr. Jones T. K. Wan of the Princeton University.

REFERENCES

- [1] K. H. Ahn and D. J. Klingenberg, *J. Rheology*, **38**, 713 (1994).
- [2] M. Ota and T. Miyamoto, *J. Appl. Phys.* **76**, 5528 (1994).
- [3] E. Lemaire, A. Meunier and G. Bossis, *J. Rheology* **39**, 1011 (1995).
- [4] D. J. Klingenberg, F. van Swol, and C. F. Zukoski, *J. Chem. Phys.* **94**, 6160 (1991).
- [5] K. W. Yu and Jones T. K. Wan, *Comput. Phys. Commun.* **129**, 177 (2000).
- [6] Y. L. Siu, Jones T. K. Wan and K. W. Yu, *Phys. Rev. E* **64**, 051506 (2001).
- [7] A. Lukkarinen and K. Kaski, *Int. J. Mod. Phys. B* **15**, 904 (2001).
- [8] J. D. Jackson, *Classical Electrodynamics* (Wiley, New York, 1975).
- [9] L. C. Davis, *J. Appl. Phys.* **72**, 1334 (1992).
- [10] Z. W. Wang, Z. F. Lin and R. B. Tao, *Int. J. Mod. Phys. B* **10**, 1153 (1996).
- [11] A. Lukkarinen and K. Kaski, *Int. J. Mod. Phys. C* **9**, 591 (1998).
- [12] C. K. Lo and K. W. Yu, *Phys. Rev. E* **64**, 031501 (2001).

FIGURES

FIG. 1. The interparticle force of the PD and DID models plotted against the reduced separation σ between two spherical particles for several dielectric contrasts, ϵ_1/ϵ_2 for one particle and ϵ'_1/ϵ_2 for the other, both in the transverse (T) and longitudinal (L) electric fields: (a) $\beta > 0, \beta' < 0$ or $\epsilon_1 > \epsilon_2 > \epsilon'_1$ and (b) $\beta = \beta' < 0$ or $\epsilon_2 > \epsilon_1 = \epsilon'_1$.

FIG. 2. The displacement-time graph for athermal aggregation of two spherical particles in a uniaxial field for various dielectric contrasts: (a) $\beta > 0, \beta' < 0$ or $\epsilon_1 > \epsilon_2 > \epsilon'_1$, (b) $\epsilon_2 > \epsilon_1 = \epsilon'_1$ in low volume fractions, and (c) $\epsilon_2 > \epsilon_1 = \epsilon'_1$ in high volume fractions.

FIG. 3. The correction factor of the aggregation time of two spherical particles in a uniaxial field plotted against the initial separation. The upper panel corresponds to the transverse field case while the lower pannel corresponds to the longitudinal field case.

FIG. 4. The displacement-time graph for athermal aggregation of two spherical particles in a rotating field for various dielectric contrasts, rotating field frequencies for (a) low volume fractions and (b) high volume fractions.

FIG. 5. The correction factor of the aggregation time of two spherical particles in a rotating field plotted against the initial separation for two different rotating field frequencies ω , and τ_{DID} and τ_{PD} are the aggregation times in the DID and PD models respectively.

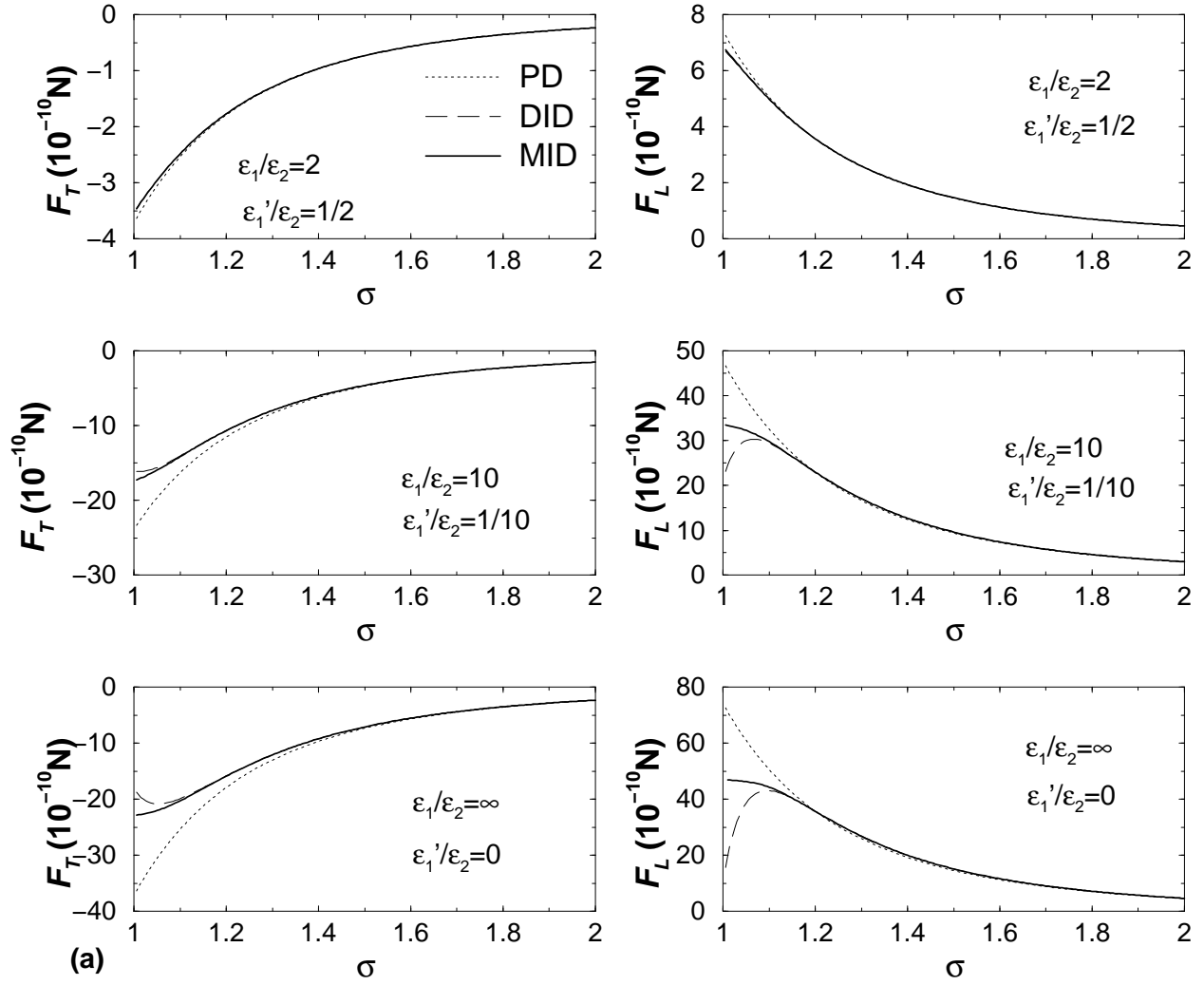


Fig.1(a)/Wong, Sun and Yu

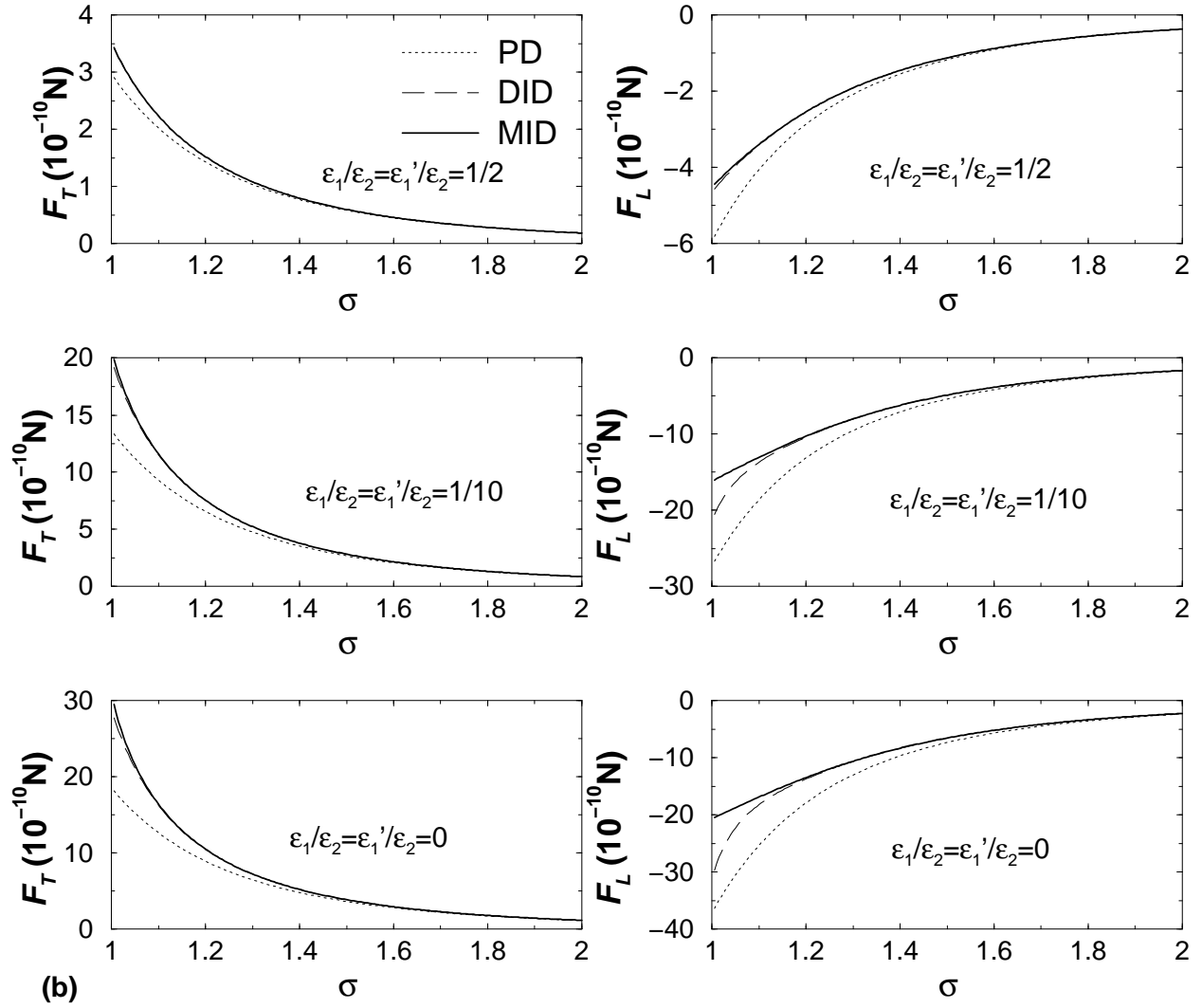


Fig.1(b)/Wong, Sun and Yu

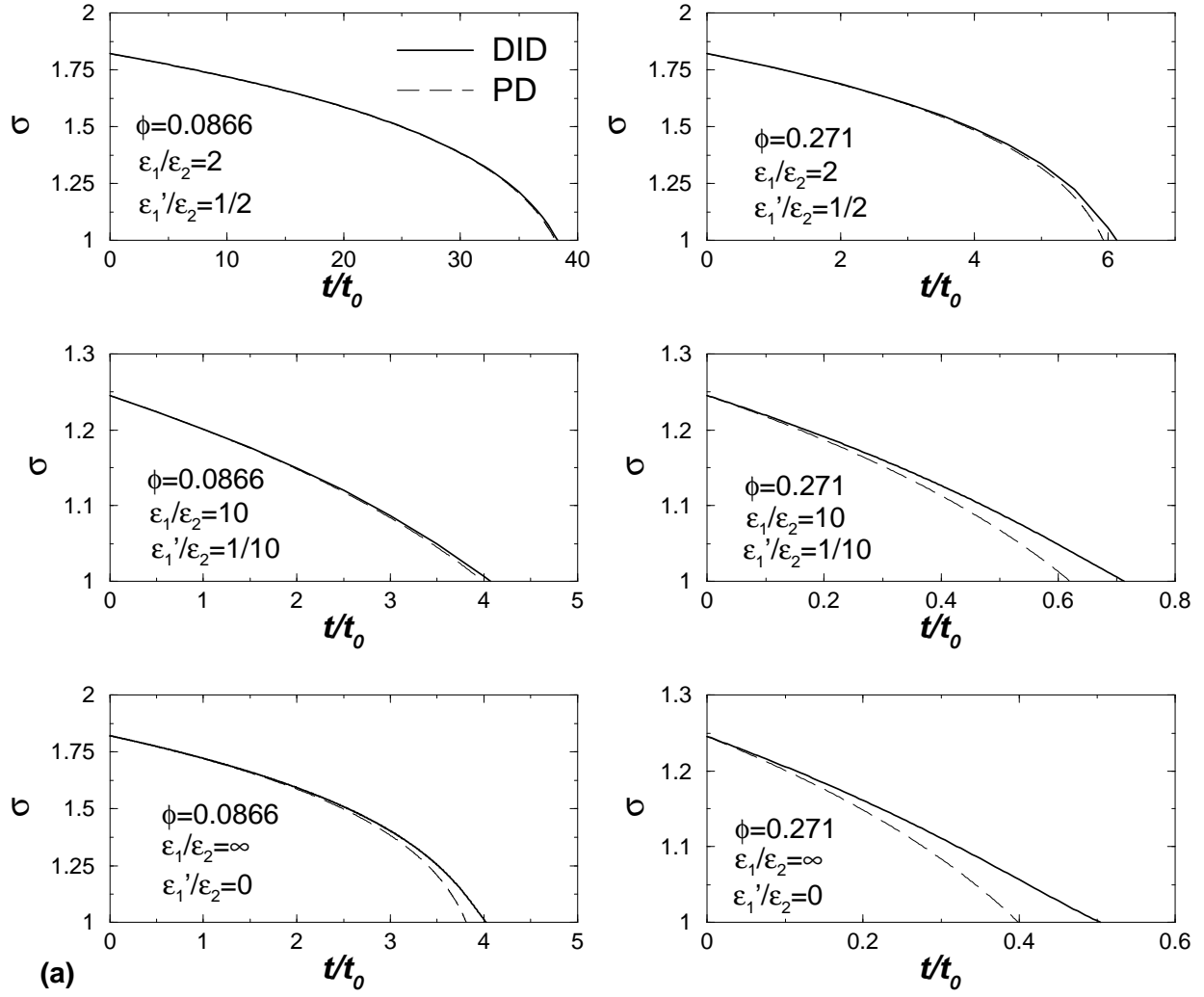


Fig.2(a)/Wong, Sun and Yu

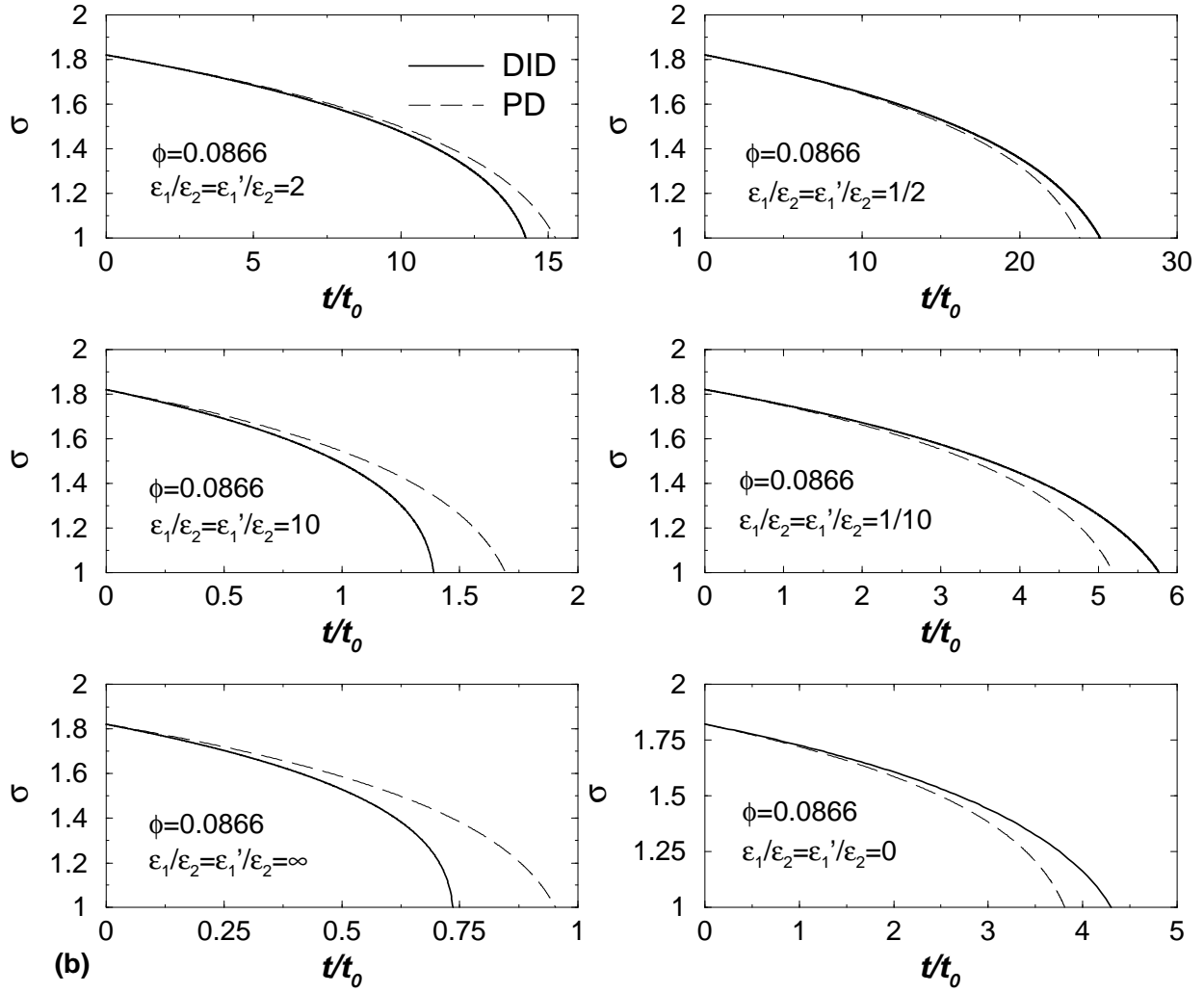


Fig.2(b)/Wong, Sun and Yu

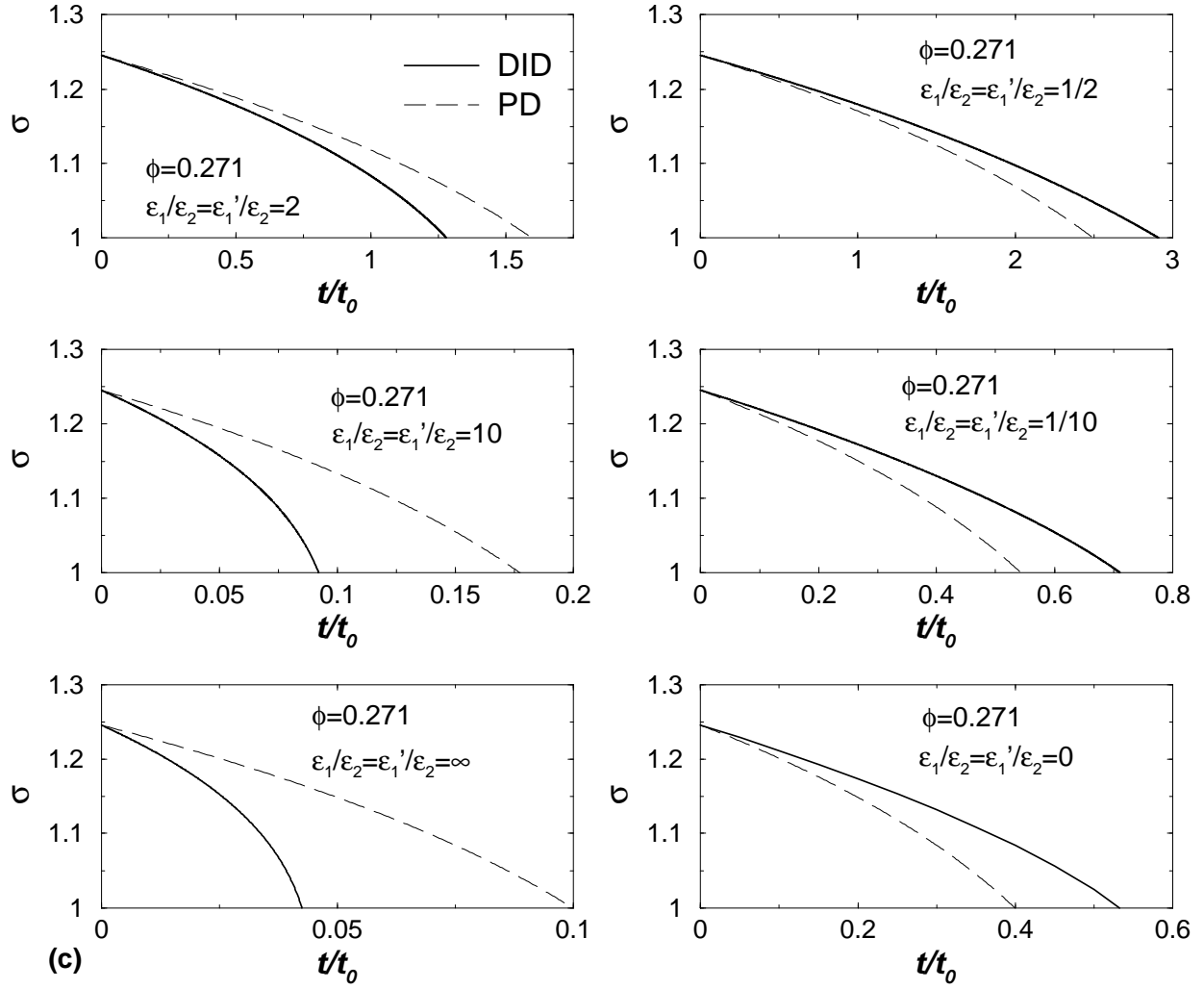


Fig.2(c)/Wong, Sun and Yu

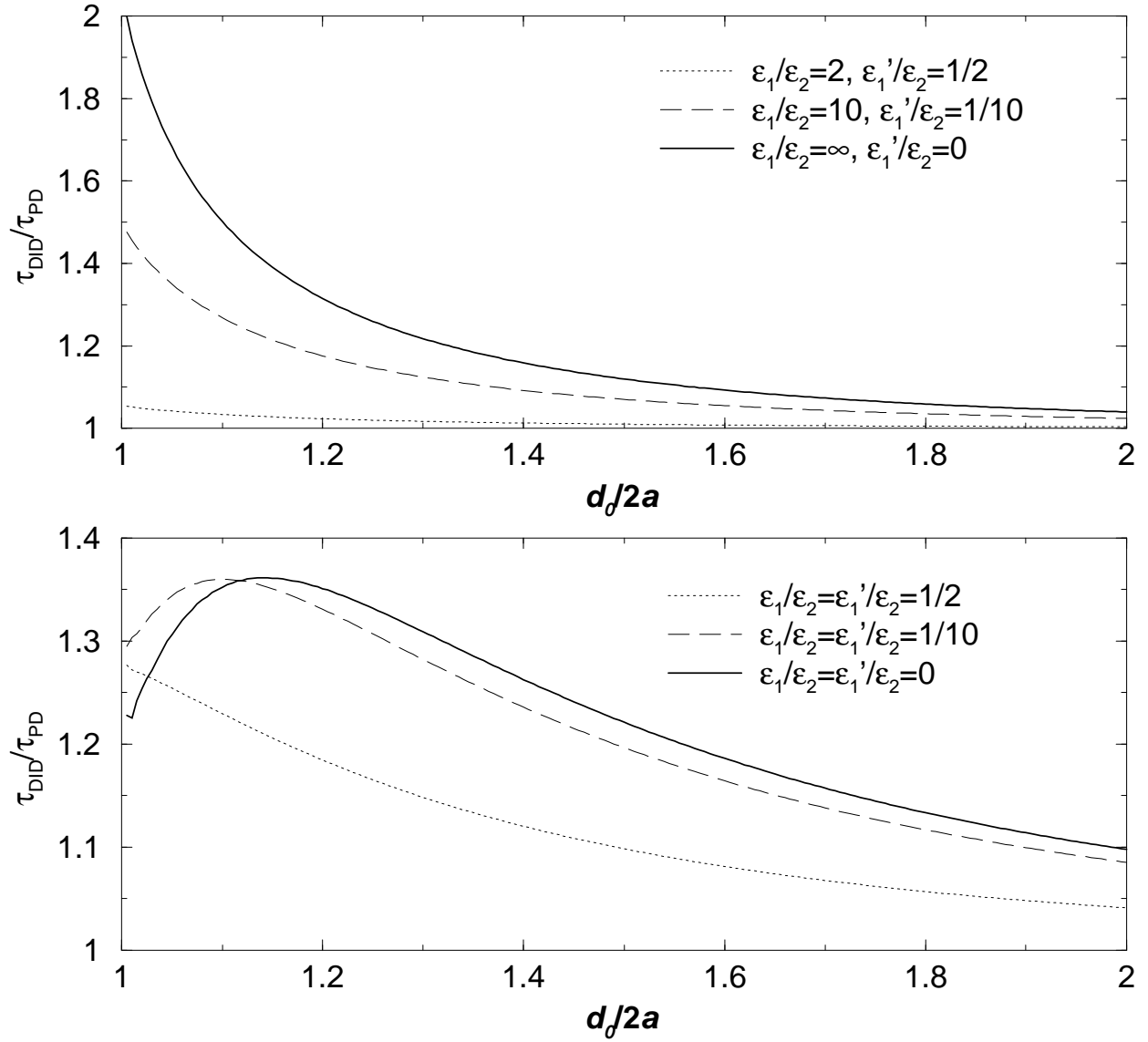


Fig.3/Wong, Sun and Yu

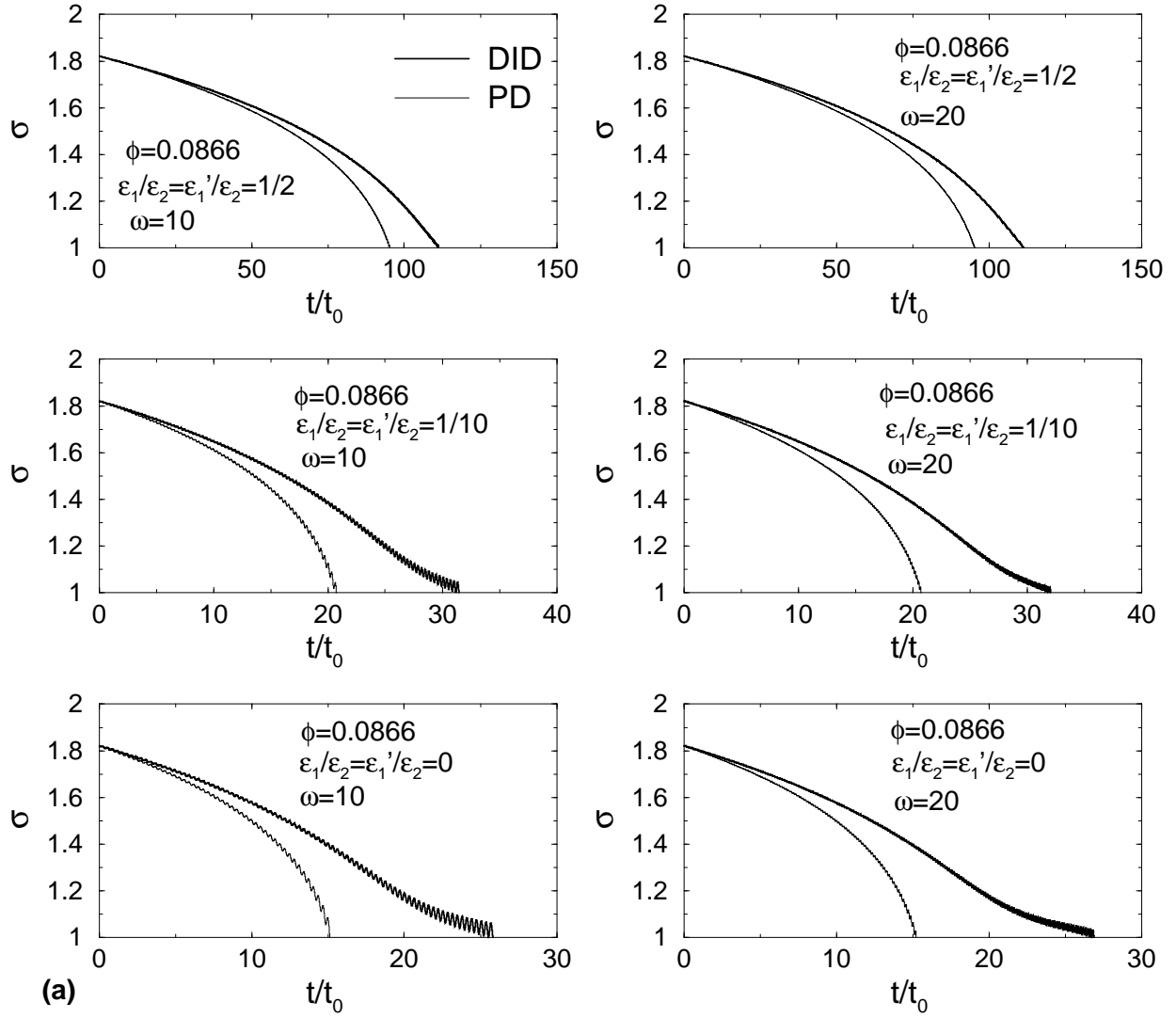


Fig.4(a)/Wong, Sun and Yu

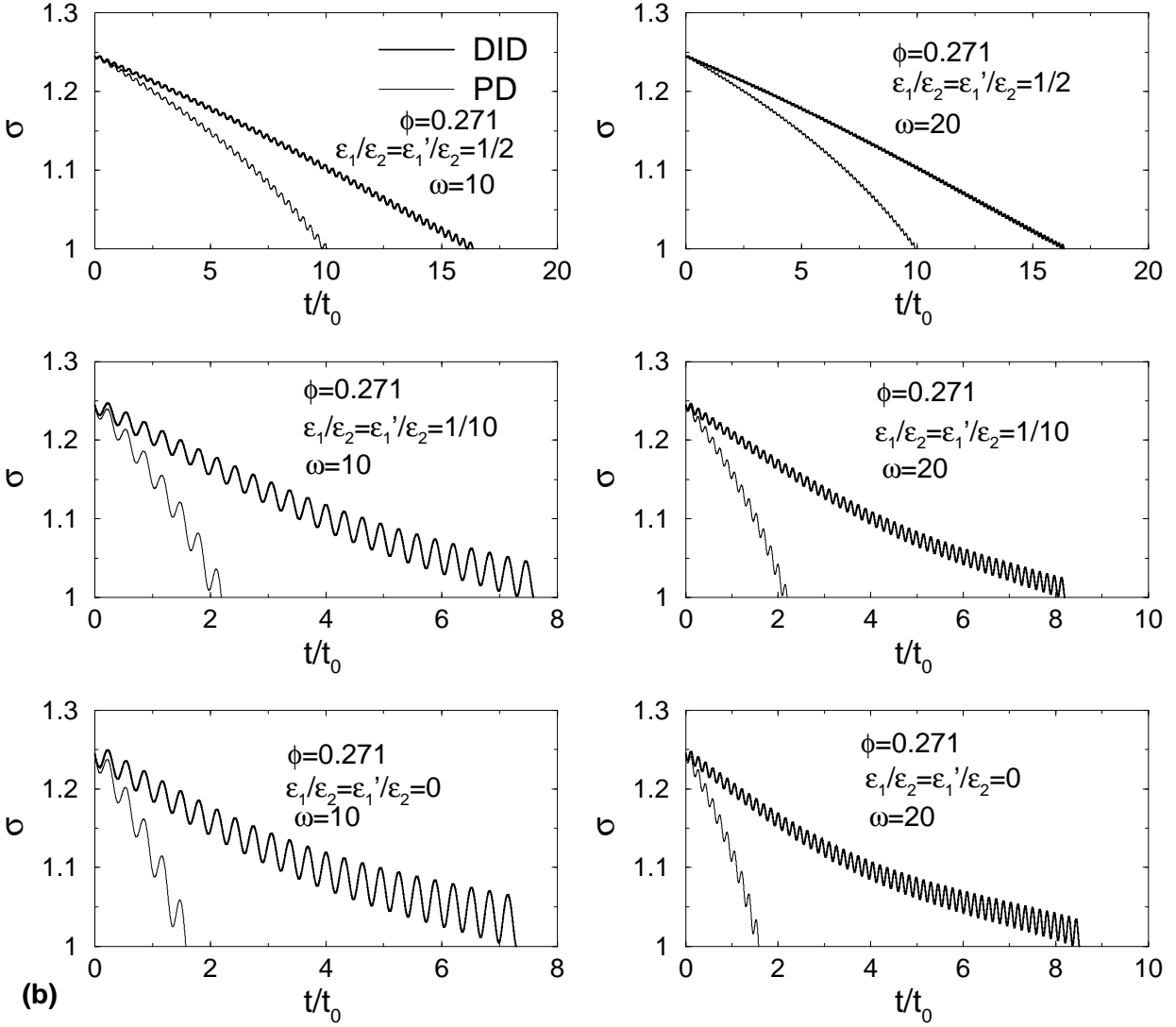


Fig.4(b)/Wong, Sun and Yu

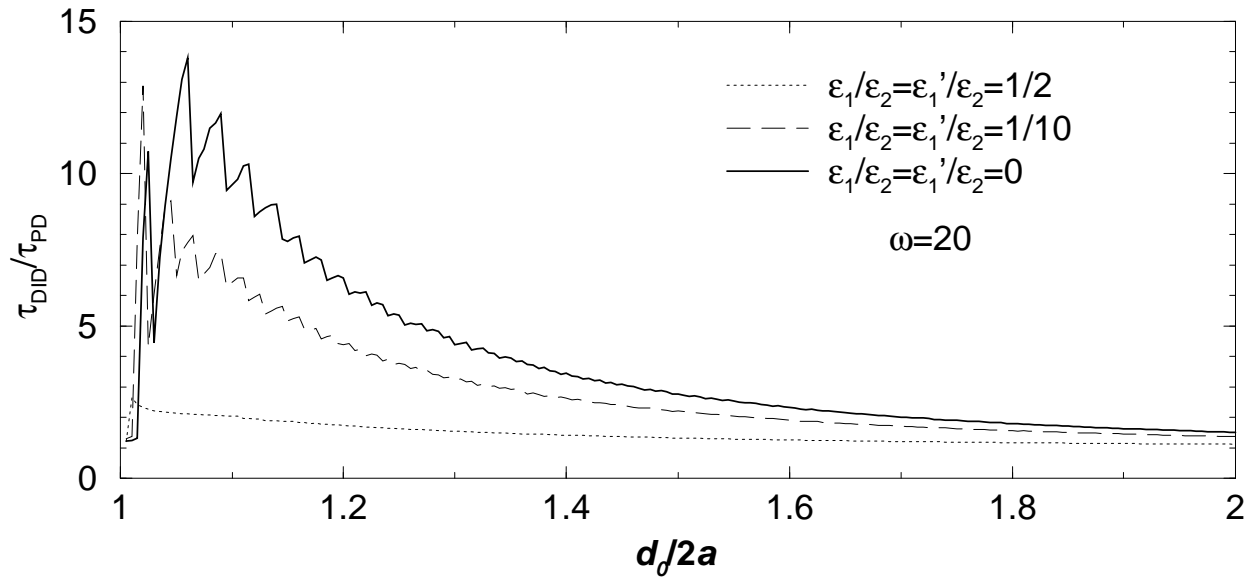
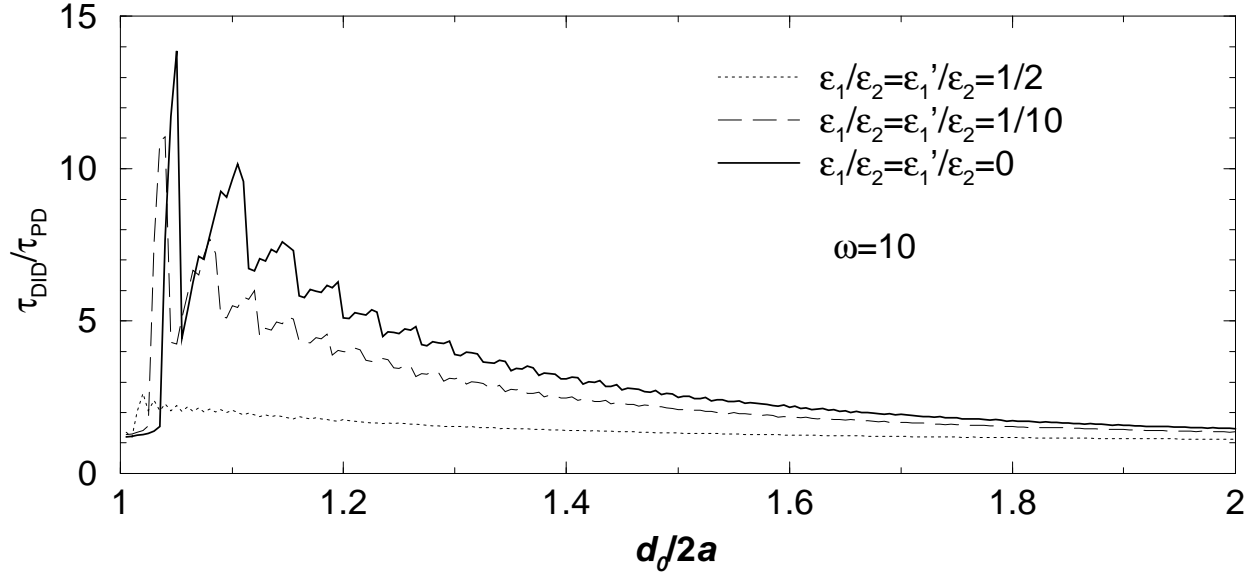


Fig.5/Wong, Sun and Yu